Modelling a rockfall field experiment using the stochastic RocPro3D software: effects of the DTM resolution

J.-D. Barnichon[1], C. Chautard[1]

[1] RocPro3D, Agreen Labo Village by CA, 4 rue Charles Sadron, 45100 Orléans, France

SUMMARY: In the context of individual rockfall simulations, the DTM is known to be a first-order factor influencing the trajectories of blocks. With available high resolution topographic surveys, the question arises as to what is the optimum DTM resolution required to perform such simulations. Based on an existing detailed field experiment and using the stochastic rockfall simulation software RocPro3D (v6.2.0), the influence of DTM resolution is investigated. The results indicate that the DTM mesh size should preferably be at least equal to the block size.

Keywords: rockfall, trajectory simulation, topography effect, RocPro3D

Introduction

Stochastic (Monte-Carlo) simulations have been used for several decades to simulate rockfall propagation (e.g. Crosta & Agliardi, 2003; Cottaz et al., 2010; Dorren et al., 2023). Most of them share a lumped-mass based formulation, in which the contact between blocks and the DTM is simplified as a unique point, and which allows the computation of very large numbers of blocks (millions and more) in a short amount of time (hours), taking into account many sources of uncertainty (Li & Lan, 2015). The effect of DTM resolution has already been studied at large scales in the past (e.g. Crosta & Agliardi, 2003). This effect is further investigated here using field experiments carried out in the Authume quarry, France (Bourrier et al., 2021).

Input data, soil mapping, and simulation

From the original raster data, a composite TIN-based mesh was generated from a Delaunay triangulation with the original raster resolution of 0.2 m. Three additional meshes were also generated to reduce this resolution (i.e., increase the size of the faces) by uniform resampling to 0.5 m, 1.0 m and 2.0 m, respectively. On these four DTM meshes, soils were mapped using a local slope criterion using the RocPro3D standard soil library parameter set (see Tab. 1 for the deterministic parameters). The resulting soil mapping is shown in Fig. 1 for the 0.5 m DTM.

Table 1. Soil mapping

Local slope [°]	Mapped soil	R_N [-]	R_T [-]	ΔR [-]	k [-]	Δk [-]
70-90	Sane rock	0.55	0.90	0.04	0.45	0.12
45-70	Altered rock	0.50	0.85	0.05	0.50	0.15
20-45	Compact debris	0.40	0.85	0.08	0.55	0.15
0-20	Loose debris	0.32	0.82	0.03	0.60	0.12

Consistent with experimental data and analysis (Bourrier et al., 2021), we introduced 2 release zones with constant block size (RZ-A and RZ-B) and 4 vertical evaluation screens (ES1-A, ES2-A, ES1-B, ES2-B), see Fig. 1. For each DTM, stochastic simulations were performed with the RocPro3D software (https://www.rocpro3d.com), using a hybrid **lumped-mass** formulation that accounts for block **rotation** (LM-R) and launching 1 million blocks per release zone, which resulted in a total CPU time between 11.8 min and 26.3 min on Intel core i5-12500H.

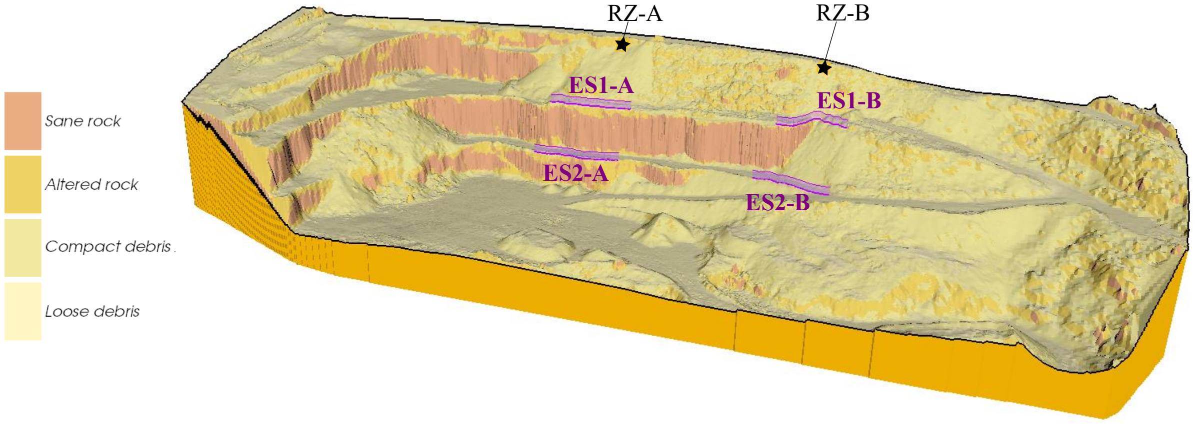

Figure 1. Full 3D view of the modelled zone and mapped soils (DTM resolution 0.5 m) - Black stars: release zones (RZ-A and RZ-B); Violet: evaluation screens ES1-A, ES2-A, ES1-B, ES2-B.

Stopping points

Observed block trajectory stopping points are shown in Fig. 2a, and computed maps (using a fixed analysis raster cell size of 1 m for all DTMs) of the number of stopping points per raster cell are shown on Figs. 2b-e. Visual analysis suggests that the computed stopping zones are broadly comparable to the field observations. However, a more detailed comparison of the medium and low-resolution maps (Figs. 2c-d-e) with the highest-resolution map (Fig. 2b) shows that the latter i) overpredicts the occurrence of stopping points in the slope immediately below RZ-A and in the access ramp below RZ-B (see solid red ellipses), and ii) underpredicts the occurrence of stopping points in the terminal slope below RZ-B (see dashed red ellipse).

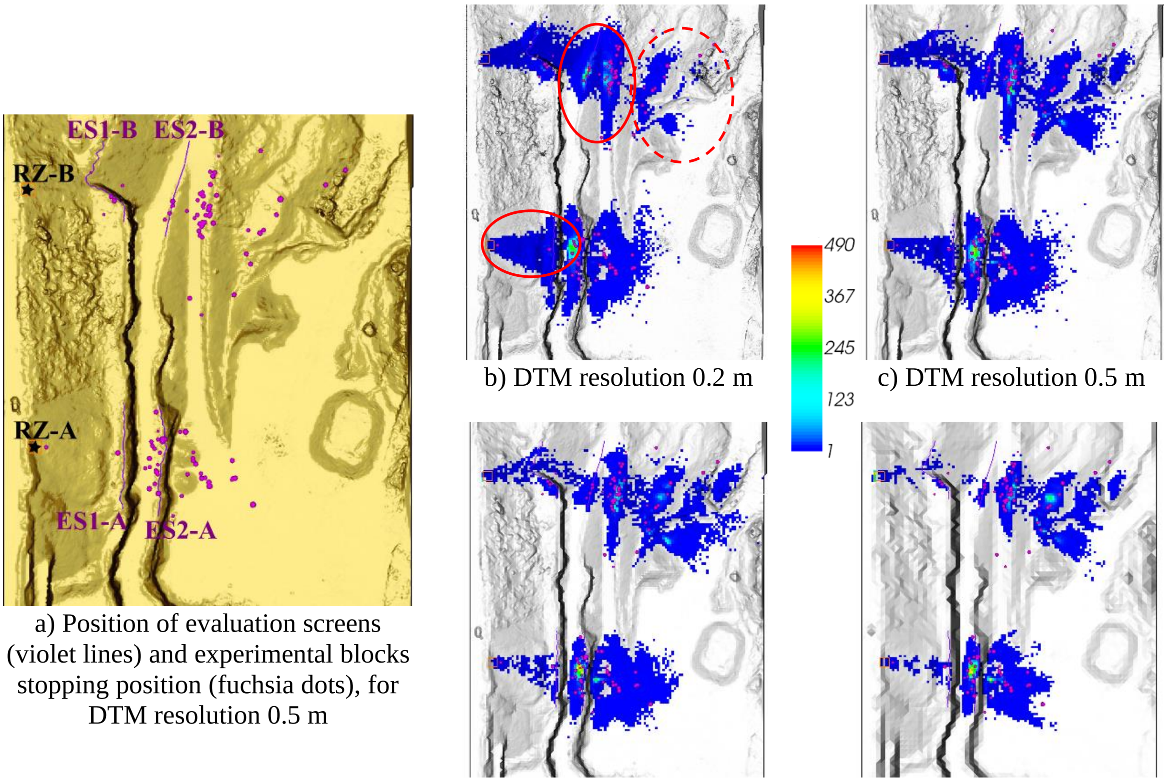

a) Position of evaluation screens (violet lines) and experimental blocks stopping position (fuchsia dots), for DTM resolution 0.5 m

b) DTM resolution 0.2 m

c) DTM resolution 0.5 m

d) DTM resolution 1.0 m

e) DTM resolution 2.0 m

Figure 2. X-Y plane view of: a) Experimental evaluation screens (violet lines) and blocks stopping position (fuschia dots), adapted from Bourrier et al. (2021); Maps of simulated number of stopping points for DTM resolution: b) 0.2 m, c) 0.5 m, d) 1.0 m, e) 2.0 m.

The highest resolution DTM (0.2 m) having a size smaller than the blocks, the perceived terrain orientation (Noël et al., 2021) could probably explain most the differences compared to lower resolution ones, as only a point contact between the blocks and the DTM is possible in the hybrid lumped-mass approach used here. With respect to the previous data, the calculation of the minimum distance (*MinDist*) between each observed block and all simulated stopping points allows to obtain quantile (Q) values (Tab. 2). As a result, the 0.5 m and 1.0 m resolutions roughly best fit observations up to Q90 (Qx: Q at x%) and are very close to minimum values for larger quantiles. This is interpreted as a result of the size of the blocks used in the field experiment (sphere equivalent diameter between 0.5 and 1.1 m), which are close to these DTM resolutions (0.5 m and 1.0 m).

Table 2. Computed *MinDist* quantile values (Qx: quantile at x%)

DTM resolution [m]	Q50 [m]	Q80 [m]	Q90 [m]	Q95 [m]	Q100 [m]
0.2	0.04	0.20	0.98	1.52	4.66
0.5	0.02	0.20	0.92	1.41	5.70
1.0	0.02	0.17	0.88	2.02	4.94
2.0	0.04	0.32	2.11	4.42	11.85

Reached distance

Cumulative Distribution Functions (CDFs) of the horizontal reached distance are shown in Fig. 3 for all DTM resolutions, together with experimental observations (Bourrier et al., 2021). The general shape of the observed CDFs compares quite well with the simulated ones, with the best fit being obtained for the 0.5 DTM at path B (orange curve in Fig. 3b). This reflects the consistent capture of the main zones of block deposition (flat zones, berms…) compared to the experimental data.

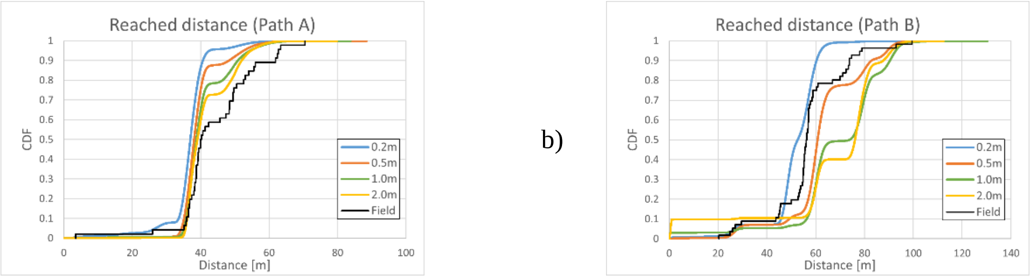

Figure 3. Reached distance CDFs (simulations and experiment) for: a) path A; b) path B.

Velocity at evaluation screens

The CDFs of translational velocities computed at ES1-A, ES2-A, ES1-B, ES2-B evaluation screens are compared with the corresponding observed CDFs in Fig. 4. For ES1-A, none of the computed CDFs reproduce the observed very low velocities (Fig. 4a), although the extreme values are well reproduced. This discrepancy could not be explained in the present simulations, as was also concluded from non-smooth dynamic simulations (Bourrier & Acary, 2022). For the other evaluation screens (ES2-A, ES1-B, ES2-B), the fit between computed and observed CDFs is well captured, especially the bimodal distribution at ES2-A (Fig. 4b) and the unimodal distribution at ES1-B (Fig. 4c). At ES2-B, the bimodal fit is not captured at intermediate velocities (Fig. 4d), although values close to extremes are well reproduced. It is noteworthy that the CDFs obtained in the present simulations, based on a hybrid lumped-mass approach that takes into account the rotational velocity (LM-R RocPro3D formulation), compare very well with CDFs obtained from non-smooth dynamic simulations (Bourrier & Acary, 2022).

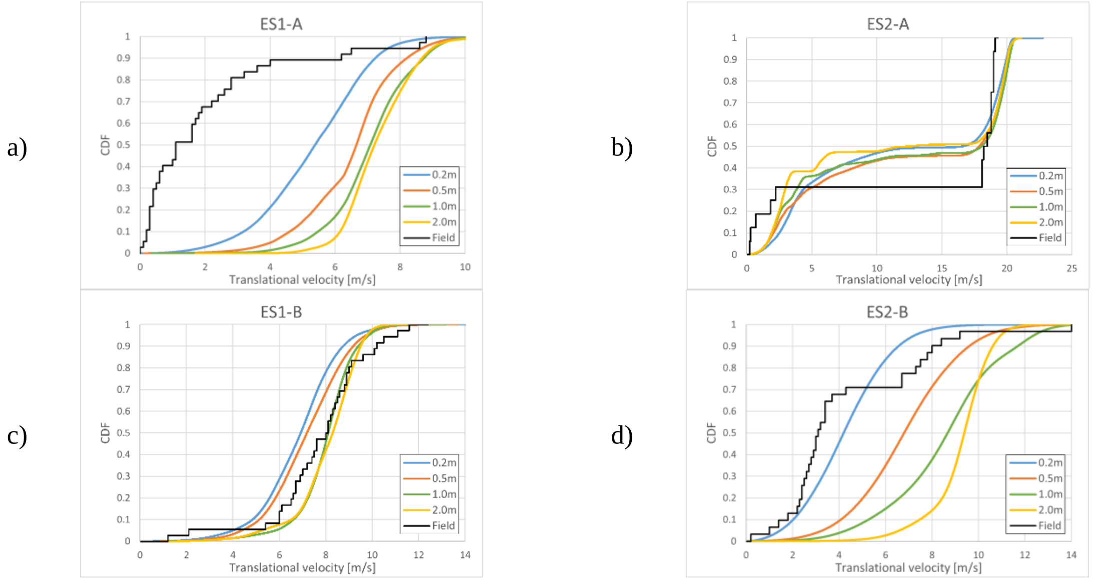

Figure 4. Translational velocities CDFs (simulations and field experiment) at each protection:
a) ES1-A; b) ES2-A; c) ES1-B; d) ES2-B.

Conclusion

The Authume field experiment was used to investigate the effect of DTM resolution, considering values smaller and larger (0.2 m to 2.0 m) than the block size (equivalent diameter between 0.5 m and 1.1 m). Notably, all simulations were performed using the RocPro3D software without modification of the standard soil parameters, using a soil mapping procedure based on local slope criteria. Analysis of the results shows that the best agreement between our hybrid LM-R based simulations and the experimental observations is obtained at DTM resolutions of 0.5 m to 1.0 m, i.e. close to the experimental block size. This is consistent with the fact that DTM accuracy is recognised as a first-order factor in rockfall modelling (Bourrier & Accary, 2022).

With respect to block size, high resolution (i.e. small mesh size) DTMs do not necessarily improve the modelling quality, especially for oversampled DTMs. In fact, in lumped-mass based simulations, they may even introduce some bias in the propagation modelling due to an over-sensitivity to the DTM rugosity (if any). Where consistent with curvatures and slopes, the DTM mesh size should preferably be at least close to the block size.

References

Bourrier F & Acary V (2022) Predictive capabilities of 2D and 3D block propagation models integrating block shape assessed from field experiments. *Rock Mechanics and Rock Engineering* **55-**2, 591–609.

Bourrier F, Toe D, Garcia B, Baroth J & Lambert S (2021) Experimental investigations on complex block propagation for the assessment of propagation models quality. *Landslides* **18**-2, 639–654.

Cottaz Y, Barnichon JD, Badertscher N & Gainon F (2010) PiR3D, an effective and user-friendly 3D rockfall simulation software: formulation and case-study application. *In*, *Rock Slope Stability Symposium*, Paris.

Crosta G & Agliardi F (2003) A methodology for physically based rockfall hazard assessment. *Natural Hazards and Earth System Sciences* **3**-5, 407–422.

Dorren L, Schaller C, Erbach A & Moos C (2023) Automated Delimitation of Rockfall Hazard Indication Zones Using High-Resolution Trajectory Modelling at Regional Scale. *Geosciences* **13**-6, 182.

Li L & Lan H (2015) Probabilistic modeling of rockfall trajectories: a review. *Bulletin of Engineering Geology and the Environment* **74**, 1163–1176.

Noël F, Cloutier C, Jaboyedoff M & Locat J (2021) Impact-detection algorithm that uses point clouds as topographic inputs for 3D rockfall simulations. *Geosciences* **11**-5, 188.